

# Calcium imaging in the optical stretcher

Markus Gyger,<sup>1,\*</sup> Daniel Rose,<sup>1</sup> Roland Stange,<sup>1</sup> Tobias Kießling,<sup>1</sup>  
Mareike Zink,<sup>1</sup> Ben Fabry,<sup>2</sup> and Josef A. Käs<sup>1</sup>

<sup>1</sup>*Institut für Experimentelle Physik I, Abteilung für Physik der Weichen Materie, Universität  
Leipzig, Linnéstr. 5, 04103 Leipzig, Germany*

<sup>2</sup>*Center for Medical Physics and Technology, Friedrich-Alexander-University of  
Erlangen-Nürnberg, Henkestrasse 91, 91052 Erlangen, Germany*

[\\*Markus.Gyger@uni-leipzig.de](mailto:Markus.Gyger@uni-leipzig.de)

**Abstract:** The Microfluidic Optical Stretcher (MOS) has previously been shown to be a versatile tool to measure mechanical properties of single suspended cells. In this study we combine optical stretching and fluorescent calcium imaging. A cell line transfected with a heat sensitive cation channel was used as a model system to show the versatility of the setup. The cells were loaded with the  $\text{Ca}^{2+}$  dye Fluo-4 and imaged with confocal laser scanning microscopy while being stretched. During optical stretching heat is transferred to the cell causing a pronounced  $\text{Ca}^{2+}$  influx through the cation channel. The technique opens new perspectives for investigating the role of  $\text{Ca}^{2+}$  in regulating cell mechanical behavior.

© 2011 Optical Society of America

**OCIS codes:** (120.6810) Thermal effects; (170.1790) Confocal microscopy; (170.2520) Fluorescence microscopy; (110.0180) Microscopy; (170.1530) Cell analysis; (170.2655) Functional monitoring and imaging; (170.3880) Medical and biological imaging; (170.4580) Optical diagnostics for medicine; (350.4855) Optical tweezers or optical manipulation.

---

## References and links

1. A. Ashkin, "Acceleration and trapping of particles by radiation pressure," *Phys. Rev. Lett.* **24**, 156–159 (1970).
2. A. Ashkin and J. Dziedzic, "Optical trapping and manipulation of viruses and bacteria," *Science* **235**, 1517–1520 (1987).
3. A. Ashkin, J. M. Dziedzic, and T. Yamane, "Optical trapping and manipulation of single cells using infrared laser beams," *Nature* **330**, 769–771 (1987).
4. K. Svoboda and S. M. Block, "Biological applications of optical forces," *Annu. Rev. Biophys. Biomol. Struct.* **23**, 247–285 (1994).
5. H. Zhang and K.-K. Liu, "Optical tweezers for single cells," *J. R. Soc., Interface* **5**, 671–690 (2008).
6. J. Guck, R. Ananthakrishnan, T. J. Moon, C. C. Cunningham, and J. Käs, "Optical deformability of soft biological dielectrics," *Phys. Rev. Lett.* **84**, 5451–5454 (2000).
7. J. Guck, R. Ananthakrishnan, H. Mahmood, T. J. Moon, C. C. Cunningham, and J. Käs, "The optical stretcher: a novel laser tool to micromanipulate cells," *Biophys. J.* **81**, 767–784 (2001).
8. J. Guck, S. Schinkinger, B. Lincoln, F. Wottawah, S. Ebert, M. Romeyke, D. Lenz, H. M. Erickson, R. Ananthakrishnan, D. Mitchell, J. Käs, S. Ulvick, and C. Bilby, "Optical deformability as an inherent cell marker for testing malignant transformation and metastatic competence," *Biophys. J.* **88**, 3689–3698 (2005).
9. F. Lautenschläger, S. Paschke, S. Schinkinger, A. Bruel, M. Beil, and J. Guck, "The regulatory role of cell mechanics for migration of differentiating myeloid cells," *Proc. Natl. Acad. Sci. U.S.A.* **106**, 15696–15701 (2009).
10. B. Lincoln, S. Schinkinger, K. Travis, F. Wottawah, S. Ebert, F. Sauer, and J. Guck, "Reconfigurable microfluidic integration of a dual-beam laser trap with biomedical applications," *Biomed. Microdevices* **9**, 703–710 (2007).
11. T. W. Remmerbach, F. Wottawah, J. Dietrich, B. Lincoln, C. Wittekind, and J. Guck, "Oral Cancer Diagnosis by Mechanical Phenotyping," *Cancer Res.* **69**, 1728–1732 (2009).
12. A. Fritsch, M. Höckel, T. Kiessling, K. D. Nnetu, F. Wetzel, M. Zink, and J. A. Käs, "Are biomechanical changes necessary for tumour progression?" *Nat. Phys.* **6**, 730–732 (2010).
13. D. Icard-Arcizet, O. Cardoso, A. Richert, and S. Hnon, "Cell stiffening in response to external stress is correlated to actin recruitment," *Biophys. J.* **94**, 2906–2913 (2008).

14. M. Whitaker, "Calcium at fertilization and in early development," *Physiol. Rev.* **86**, 25–88 (2006).
15. E. Neher and T. Sakaba, "Multiple roles of calcium ions in the regulation of neurotransmitter release," *Neuron* **59**, 861–872 (2008).
16. J. Lee, A. Ishihara, G. Oxford, B. Johnson, and K. Jacobson, "Regulation of cell movement is mediated by stretch-activated calcium channels," *Nature* **400**, 382–386 (1999).
17. R. E. Haddock and C. E. Hill, "Rhythmicity in arterial smooth muscle," *J. Physiol.* **566**, 645–656 (2005).
18. G. Iribe, C. W. Ward, P. Camelliti, C. Bollensdorff, F. Mason, R. A. Burton, A. Garny, M. K. Morphew, A. Hoenger, W. J. Lederer, and P. Kohl, "Axial stretch of rat single ventricular cardiomyocytes causes an acute and transient increase in Ca<sup>2+</sup> spark rate," *Circ. Res.* **104**, 787–795 (2009).
19. C. Wei, X. Wang, M. Chen, K. Ouyang, L.-S. Song, and H. Cheng, "Calcium flickers steer cell migration," *Nature* **457**, 901–905 (2009).
20. S. Wray, "Insights into the uterus," *Exp. Physiol.* **92**, 621–631 (2007).
21. M. J. Sanderson and E. R. Dirksen, "Mechanosensitivity of cultured ciliated cells from the mammalian respiratory tract: implications for the regulation of mucociliary transport," *Proc. Natl. Acad. Sci. U.S.A.* **83**, 7302–7306 (1986).
22. M. J. Sanderson, A. C. Charles, and E. R. Dirksen, "Mechanical stimulation and intercellular communication increases intracellular Ca<sup>2+</sup> in epithelial cells," *Cell Regul.* **1**, 585–596 (1990).
23. R. Y. Tsien, "New calcium indicators and buffers with high selectivity against magnesium and protons: design, synthesis, and properties of prototype structures," *Biochemistry* **19**, 2396–2404 (1980).
24. R. Y. Tsien, "A non-disruptive technique for loading calcium buffers and indicators into cells," *Nature* **290**, 527–528 (1981).
25. R. Y. Tsien, T. Pozzan, and T. J. Rink, "Calcium homeostasis in intact lymphocytes: cytoplasmic free calcium monitored with a new, intracellularly trapped fluorescent indicator," *J. Cell Biol.* **94**, 325–334 (1982).
26. A. Minta, J. Kao, and R. Tsien, "Fluorescent indicators for cytosolic calcium based on rhodamine and fluorescein chromophores," *J. Biol. Chem.* **264**, 8171–8178 (1989).
27. K. R. Gee, K. A. Brown, W.-N. U. Chen, J. Bishop-Stewart, D. Gray, and I. Johnson, "Chemical and physiological characterization of fluo-4 Ca<sup>2+</sup>-indicator dyes," *Cell Calcium* **27**, 97–106 (2000).
28. R. M. Paredes, J. C. Etzler, L. T. Watts, W. Zheng, and J. D. Lechleiter, "Chemical calcium indicators," *Methods* **46**, 143–151 (2008).
29. A. E. Palmer and R. Y. Tsien, "Measuring calcium signaling using genetically targetable fluorescent indicators," *Nat. Protoc.* **1**, 1057–1065 (2006).
30. N. Demaurex, "Calcium measurements in organelles with Ca<sup>2+</sup>-sensitive fluorescent proteins," *Cell Calcium* **38**, 213–222 (2005).
31. M. J. Caterina and D. Julius, "The vanilloid receptor: a molecular gateway to the pain pathway," *Annu. Rev. Neurosci.* **24**, 487–517 (2001).
32. M. J. Caterina, "Transient receptor potential ion channels as participants in thermosensation and thermoregulation," *Am. J. Physiol. Regulatory Integrative Comp. Physiol.* **292**, R64–R76 (2007).
33. B. Nilius, G. Owsianik, T. Voets, and J. A. Peters, "Transient receptor potential cation channels in disease," *Physiol. Rev.* **87**, 165–217 (2007).
34. M. Caterina, M. Schumacher, M. Tominaga, T. Rosen, J. Levine, and D. Julius, "The capsaicin receptor: a heat-activated ion channel in the pain pathway," *Nature* **389**, 816–824 (1997).
35. M. Tominaga, M. J. Caterina, A. B. Malmberg, T. A. Rosen, H. Gilbert, K. Skinner, B. E. Raumann, A. I. Basbaum, and D. Julius, "The cloned capsaicin receptor integrates multiple pain-producing stimuli," *Neuron* **21**, 531–543 (1998).
36. J. B. Davis, J. Gray, M. J. Gunthorpe, J. P. Hatcher, P. T. Davey, P. Overend, M. H. Harries, J. Latcham, C. Clapham, K. Atkinson, S. A. Hughes, K. Rance, E. Grau, A. J. Harper, P. L. Pugh, D. C. Rogers, S. Bingham, A. Randall, and S. A. Sheardown, "Vanilloid receptor-1 is essential for inflammatory thermal hyperalgesia," *Nature* **405**, 183–187 (2000).
37. L. A. Birder, "More than just a barrier: urothelium as a drug target for urinary bladder pain," *Am. J. Physiol.* **289**, F489–F495 (2005).
38. C.-K. Park, M. S. Kim, Z. Fang, H. Y. Li, S. J. Jung, S.-Y. Choi, S. J. Lee, K. Park, J. S. Kim, and S. B. Oh, "Functional Expression of thermo-transient receptor potential channels in dental primary afferent neurons," *J. Biol. Chem.* **281**, 17304–17311 (2006).
39. M. Madou, *Fundamentals of Microfabrication: The Science of Miniaturization* (CRC Press, 2002).
40. S. Ebert, K. Travis, B. Lincoln, and J. Guck, "Fluorescence ratio thermometry in a microfluidic dual-beam laser trap," *Opt. Express* **15**, 15493–15499 (2007).
41. M. St. Pierre, P. Reeh, and K. Zimmermann, "Differential effects of trpv channel block on polymodal activation of rat cutaneous nociceptors in vitro," *Exp. Brain Res.* **196**, 31–44 (2009).
42. J. R. Savidge, S. P. Ransinghe, and H. P. Rang, "Comparison of intracellular calcium signals evoked by heat and capsaicin in cultured rat dorsal root ganglion neurons and in a cell line expressing the rat vanilloid receptor, vr1," *Neuroscience* **102**, 177–184 (2001).
43. M. L. Woodruff, A. P. Sampath, H. R. Matthews, N. V. Krasnoperova, J. Lem, and G. L. Fain, "Measurement

- of cytoplasmic calcium concentration in the rods of wild-type and transducin knock-out mice," *J. Physiol.* **542**, 843–854 (2002).
44. H. Schmidt, K. M. Stiefel, P. Racay, B. Schwaller, and J. Eilers, "Mutational analysis of dendritic  $Ca^{2+}$  kinetics in rodent purkinje cells: role of parvalbumin and calbindin d28k," *J. Physiol.* **551**, 13–32 (2003).
  45. F. Wetzel, S. Röncke, K. Müller, M. Gyger, D. Rose, M. Zink, and J. Ks, "Single cell viability and impact of heating by laser absorption," *Eur. Biophys. J.* **40**, 1–6 (2011).
  46. C. T. Mierke, D. Rösel, B. Fabry, and J. Brábek, "Contractile forces in tumor cell migration," *Eur. J. Cell Biol.* **87**, 669–676 (2008).
  47. B. Fabry, G. N. Maksym, J. P. Butler, M. Glogauer, D. Navajas, and J. J. Fredberg, "Scaling the microrheology of living cells," *Phys. Rev. Lett.* **87**, 148102 (2001).
  48. F. Wottawah, S. Schinkinger, B. Lincoln, R. Ananthakrishnan, M. Romeyke, J. Guck, and J. Käs, "Optical rheology of biological cells," *Phys. Rev. Lett.* **94**, 098103 (2005).
  49. R. Ananthakrishnan, J. Guck, F. Wottawah, S. Schinkinger, B. Lincoln, M. Romeyke, T. Moon, and J. Käs, "Quantifying the contribution of actin networks to the elastic strength of fibroblasts," *J. Theor. Biol.* **242**, 502–516 (2006).
  50. P. Kollmannsberger and B. Fabry, "Linear and nonlinear rheology of living cells," *Annu. Rev. Mater. Res.* **41**, 75–97 (2011).
- 

## 1. Introduction

Laser based cell analysis is one of the fastest growing areas in medical technologies and has many applications in biology and biophysics. Optical traps [1–3] have become a common tool to manipulate and probe biological cells [4–9]. The Optical Stretcher, a device to micromanipulate single suspended cells, was introduced by Guck *et al.* [6, 7]. A number of applications and improvements to the setup, such as the integration of the Optical Stretcher into microfluidics, the so called Microfluidic Optical Stretcher (MOS), have been published [10–12]. The MOS was used to show for example that oral squamous carcinoma cells are more compliant and show a larger variability than cells from healthy donors [11].

As most optical trapping techniques are performed in commercially available microscopes, combination with fluorescent imaging is straight forward. Icard-Arcizet *et al.* combined optical tweezers microrheology with epifluorescence microscopy of GFP-actin and could show that the strengthening of the probed focal adhesions correlated with a recruitment of actin around the attached bead [13]. In contrast to the tweezers setup, in the Optical Stretcher the optically induced forces act directly on the surface of the suspended cell superseding the attachment of beads to the surface [6, 7]. In this study we combine intracellular  $Ca^{2+}$  imaging with measurements of cellular mechanics.

Calcium ions are among the most important messengers within the signal transduction cascade in biological cells.  $Ca^{2+}$  signaling is involved in numerous physiologically relevant processes [14–17]. It can act locally *e.g.* in so called sparks [17, 18] or flickers [19], or propagate through the cell in waves [20] that can travel via gap junctions to neighboring cells [21, 22].

Intracellular  $Ca^{2+}$  measurements require a suitable indicator [23–26]. A great variety of chemical  $Ca^{2+}$  indicators [27, 28] and the possibility to genetically encode indicators specific for addressing cellular compartments or for performing long term measurements [29, 30] has led to a great enhancement in understanding of intracellular  $Ca^{2+}$  signaling. In this study we combine optical trapping and  $Ca^{2+}$  imaging, employing a simple cell loading with Fluo-4,AM. More sophisticated  $Ca^{2+}$  imaging approaches such as genetically encoded indicators, *e.g.* targeting specific sub-cellular compartments, can be readily implicated without further modification of the setup. To show the versatility of our setup, we use HEK293 cells stably transfected with the transient receptor potential cation channel subfamily member vanilloid 1 (TRPV1) as model system.

The TRPV1, previously also referred to as vanilloid receptor 1 (VR1), is one of the best-studied members of the family of temperature-activated transient receptor potential ion channels (see [31–33] for reviews). It is slightly selective for  $Ca^{2+}$  over other extracellular cations [34].

Well-known activators of TRPV1 are heat, protons and capsaicin, the pungent compound in hot chili peppers [34, 35]. The heat response in TRPV1 transfected HEK293 cells were shown to desensitize by repeated stimulus application [34]. TRPV1 channels are involved in the pathogenesis of several diseases such as thermal hyperalgesia [36], bladder disease [37], and pain in general, *e.g.* tooth pain [38]. This makes the channel interesting as a possible target for drug treatment [33]. Here we take advantage of the fact that the ion channel is activated directly by the heating caused by the optical stretching.

## 2. Methods

### 2.1. Combination of optical stretching and confocal imaging

The Microfluidic Optical Stretcher setup was built with slight modifications as described in [10]. Instead of the glass slide used by Lincoln *et al.*, the SU-8 photoresist (MicroChem Corp., Newton, Massachusetts) was deposited by a standard photolithographic method [39] on a 100  $\mu\text{m}$  cover slip sustained by an 1 mm thick aluminum plate with a 7 mm hole in the center (Fig. 1c). This reduced the distance between the lower glass boundary and the cell allowing for the use of a 63x high NA (1.40) oil-immersion objective. The setup was mounted on a confocal laser scanning microscope (CLSM, Leica TCS SP2, Leica, Wetzlar, Germany). A custom made light weight aluminum stage, meeting the weight requirements of the piezo z-stage of the CSLM, was used for computer controlled adjustment of the height of the focal plane. The setup is shown in Fig. 1. The main advantage of using a CLSM is the possibility to observe a bright-field and a fluorescence image at the same time without slow filter cube exchange and illumination adjustment. Additionally it is possible without further modifications of the setup to obtain 3D images of trapped cells, this however is possible only for slow processes as the recording of such a stack of images is time consuming.

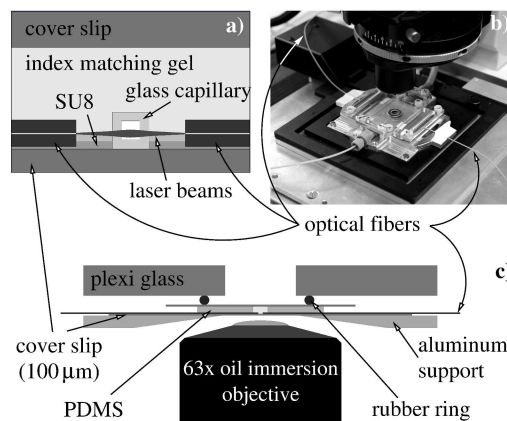


Fig. 1. Schematic cross section along the laser fibers (a,c) and photo (b) of the Optical Stretcher setup mounted on the piezo driven z-stage of the CLSM. a) magnification of the Stretcher chamber, details can be found in [10]. c) The SU-8 structure sustaining the optical fibers was spin-coated on a 100  $\mu\text{m}$  glass cover slip, supported by a stable aluminum structure. This reduced the distance between lower glass boundary and the trap position of cell compared to the setup described by Lincoln *et al.* sufficiently such that the working distance of the oil immersion objective sufficed to observe the mid-plane of the cell.

Cells were moved into the trap region by hydrostatic pressure control. After stopping the

flow, the cells were trapped at 100 mW per fiber with two counter propagating beams emerging from a 1064 nm single mode CW Ytterbium fiber laser (YLD-10-1064, IPG Photonics, Oxford, Massachusetts) equipped with a beam splitter. Cells were stretched at 700 mW per fiber for 5 s followed by a relaxation phase at trapping power of 30 s. Three successive stretches were performed for each cell. Fluorescent images were obtained by scanning the mid-plane of the cell with a 488 nm laser, recording the emitted light between 500 and 530 nm. Images of  $43.36 \times 25.58 \mu\text{m}^2$  were taken with a resolution of  $5.90 \mu\text{m}$  per pixel at 2.75 fps. Simultaneously an additional 543 nm laser was used to obtain transmission mode images with a transmitted light detector. These images were employed to position the cell into the trap region and to assure that the flow was stopped during the measurements.

The laser was controlled via custom written Labview (National Instruments, Austin, Texas) software. It was synchronized with the images recorded with the commercial software of the CLSM using the trigger signal from the CLSM, digitalized via a NI USB-6008 (National instruments, Austin, Texas).

To correlate  $\text{Ca}^{2+}$  signaling with cellular mechanical properties, cells were measured in the MOS as described in [10]. Cells were stretched with 700 mW for 5 s as specified above. Images were recorded at 30 fps with phase contrast microscopy. The cell edge was detected for every frame from the phase contrast images and the relative deformation, *i.e.* the change of the length of the cell's axis along the laser beam during the stretch divided by the diameter of the unstretched cell, was calculated.

## 2.2. Cell culture

Human embryonic kidney cells (HEK293) stably transfected with the TRPV1 ion channel, were kindly provided by David Julius, University of California, San Francisco (UCSF). The introduction of the TRPV1 ion channel provides a inherently controllable switch for the  $\text{Ca}^{2+}$  signal.

The cells were cultured in Dulbecco's Modified Eagle Medium (PAA Laboratories GmbH, Pasching, Austria) containing 10% Fetal Calf Serum (PAA Laboratories GmbH, Pasching, Austria), 1% Penicillin-Streptomycin (PAA Laboratories GmbH, Pasching, Austria) and 0.02% G418 Disulphate salt solution (50 mg G418 salt per ml, Sigma-Aldrich, St. Louis, Missouri).

Prior to the dye loading the cells were washed with Phosphate Buffer Saline solution (PBS, Invitrogen Corporation, Carlsbad, California) to remove traces of serum that contains Trypsin inhibitor. The cells were then detached by application of 1 ml 0.025% Trypsin-EDTA (PAA Laboratories GmbH, Pasching, Austria) for 4 min. Subsequently the Trypsin was deactivated by addition of 5 ml growth medium followed by a centrifugation for 4 min at 800 rpm.

## 2.3. Dye and chelator loading of the cells

For the calcium imaging we used the fluorescent calcium dye Fluo-4,AM (Invitrogen Corporation, Carlsbad, California) [27]. The measurable  $\text{Ca}^{2+}$  concentration is in the range of 100 nM to 1 mM and the 488 nm laser of the CSLM lies in the excitation range of the dye.

Calcium chelators competitively bind  $\text{Ca}^{2+}$  ions inside the cell. The messenger  $\text{Ca}^{2+}$  is hindered to interact with its natural binding partners such as receptors and pumps, hence the signal cascade is interrupted.  $\text{Ca}^{2+}$  dyes, such as Fluo-4, act as chelators, additionally the non-fluorescent chelator BAPTA,AM (PromoCell, Heidelberg, Germany) was used in this study.

Fluo-4 and BAPTA were loaded into the cell using the acetoxymethyl ester form, a membrane permeable molecule, that is de-esterified by intracellular esterases, activating it and making it membrane impermeable.

A stock solution of a concentration of 1  $\mu\text{g}$  Fluo-4,AM per ml anhydrous Dimethyl sulfoxide (DMSO, Fluka/Sigma-Aldrich, St. Louis, Missouri) was prepared. For the Fluo-4 measure-

ments this stock solution was dissolved in PBS giving 1 ml solution at a concentration of 1  $\mu\text{M}$  Fluo-4,AM. To facilitate dye loading and reduce compartmentalization 1.1  $\mu\text{l}$  of a Pluronic F127 solution in 20% DMSO (PromoCell, Heidelberg, Germany) was added. In this solution the cell pellet was resuspended by gentle pipetting. Cells were incubated at 29–30°C for 15 min while gently stirred to prevent re-attachment.

For the measurements of cells loaded with BAPTA and Fluo-4 a stock solution of BAPTA,AM was prepared under Nitrogen atmosphere to avoid decaying of the BAPTA,AM due to moisture. BAPTA,AM was dissolved at a concentration of 12.5  $\mu\text{g}$  per ml DMSO. The cells were resuspended in 1 ml PBS solution containing 20  $\mu\text{M}$  BAPTA,AM, 1  $\mu\text{M}$  Fluo-4,AM, and 1.1  $\mu\text{l}$  of the Pluronic F127 solution in 20% DMSO. Cells were incubated at 29–30 °C for 30 min.

After incubation the AM-ester solutions were removed by centrifugation as described above and cells were resuspended in a calcium imaging buffer (CIB) consisting of 6 mM KCl (Roth, Karlsruhe, Germany), 134 mM NaCl, 1 mM  $\text{MgCl}_2$ , 2.5 mM  $\text{CaCl}_2$ , 10 mM p-(+)-Glucose, 10 mM Hepes (all from Sigma-Aldrich, St. Louis, Missouri). The pH was adjusted to 7.45 with NaOH (Sigma-Aldrich, St. Louis, Missouri). For  $\text{Ca}^{2+}$  free measurements a calcium free Imaging Buffer (CfIB) was used replacing the  $\text{CaCl}_2$  by 10  $\mu\text{M}$  EGTA (Fluka/Sigma-Aldrich, St. Louis, Missouri). In an other incubation step of 20–30 min at 21–23 °C the cells were allowed to activate the AM-esters by unspecific intracellular esterases.

To saturate the calcium dye for control experiments 1  $\mu\text{M}$  of the calcium ionophore Ionomycin (Invitrogen Corporation, Carlsbad, California) was added to a suspension of Fluo-4 and BAPTA loaded cells in CIB before the start of the experiments. Control experiments testing for the involvement of stretch-activated  $\text{Ca}^{2+}$  channels (SAC) were performed with 10  $\mu\text{M}$   $\text{GdCl}_3$  (Sigma-Aldrich, St. Louis, Missouri) and the TRPV1 channel was blocked by 10  $\mu\text{M}$  Ruthenium Red (RuR, Sigma-Aldrich, St. Louis, Missouri).

#### 2.4. Temperature measurement in the MOS

The temperature inside the trap and during the stretch was measured as described in [40]. In brief: The fluorescence ratio of the temperature sensitive dye Rhodamin-B (Fluka/Sigma-Aldrich, St. Louis, Missouri) to the temperature insensitive dye Rhodamin-110 (Fluka/Sigma-Aldrich, St. Louis, Missouri) illuminated with 488 nm was measured for three consequent stretches with the same time and power parameters as for the cell experiments. To this end a plane of size  $11.51 \times 5.93 \mu\text{m}^2$  in the center of the trap was scanned with 16.4 fps in the CLSM. The intensity ratio of the dyes was then calibrated in a custom build chamber for a temperature range of 22 to 40 °C with steps of 2 °C, whereby the temperature was controlled with a water reservoir. This calibration was performed using the same parameters for the imaging as described above. The background offset of this measurements was normalized to room temperature as follows: The mean intensity ratio during trapping at 100 mW was calculated from an average of 82 frames (5 s) before the start of each of the stretches. The intensity ratio at maximal temperature at 700 mW was determined from an average of the last 41 frames (2.5 s) of the stretches. To obtain an absolute temperature scale a linear increase with laser power was assumed. The ambient temperature, measured to be  $(23.0 \pm 0.2)$  °C, was used as a base line.

### 3. Results and discussion

#### 3.1. Simultaneous optical stretching and $\text{Ca}^{2+}$ imaging

HEK293 cells, transfected with the heat activated TRPV1 channel and loaded with the fluorescent  $\text{Ca}^{2+}$  dye Fluo-4 were optically stretched for 5 s at 700 mW per fiber while the fluorescence signal was recorded with confocal laser scanning microscopy. Images of dim (low  $\text{Ca}^{2+}$  con-

centration) and bright (high  $\text{Ca}^{2+}$  concentration) fluorescent cells can be seen in Fig. 2 (videos are available online: ([Media 1](#)), ([Media 2](#))).

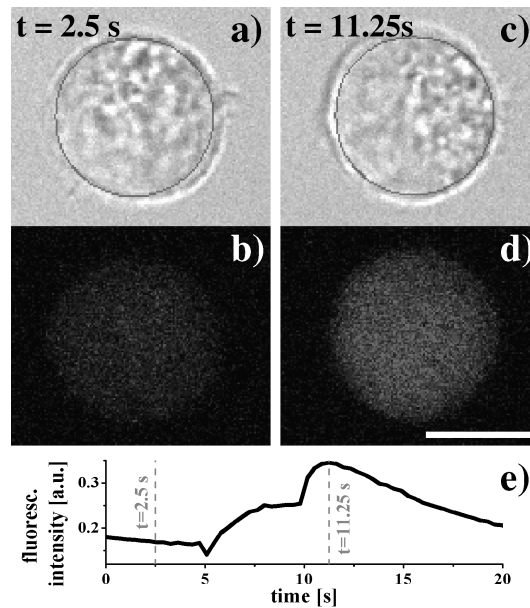


Fig. 2. Fluorescent signal (b,d) and bright-field image (a,c) of a trapped cells. The signal of the cell's mid-plane was recorded with a confocal laser scanning microscope. The fluorescence was averaged over a disk lying well inside the cell indicated by the gray circle in a) and c) to avoid artifacts due to the deformation of the cell upon stretching. e) shows the time course of the averaged fluorescent signal. Videos are available online: ([Media 1](#)), ([Media 2](#)).

In Fig. 3 typical graphs of the fluorescence signals of a) a Fluo-4 loaded cell, b) a cell co-loaded with Fluo-4 and the calcium chelator BAPTA are presented. Fig. 3 c) shows a cell loaded with Fluo-4 and BAPTA; before the measurement  $10 \mu\text{M}$  RuR, a blocker of the TRPV1 channel [41, 42], was added to the cell suspension. In all three cases the fluorescence intensity drops immediately after increasing the laser power. This results in a momentary dip for the BAPTA free case (Fig. 2e and Fig. 3a) and a lower intensity during the whole period of high laser power application for the experiments using  $20 \mu\text{M}$  BAPTA,AM (Fig. 3b and c). This effect can be explained by the temperature dependent fluorescence of Fluo-4. According to measurements of Woodruff *et al.* the maximum fluorescence of the dye falls up to one third when the temperature is increased from  $20^\circ\text{C}$  to  $37^\circ\text{C}$  [43]. To demonstrate the effect of temperature changes on the fluorescence of Fluo-4 inside the cytoplasm, cells were loaded with Fluo-4 and BAPTA as described above and measured while exposed to  $1 \mu\text{M}$  Ionomycin, a ionophore that transports  $\text{Ca}^{2+}$  ions through the plasma membrane. This way the  $\text{Ca}^{2+}$  dye was saturated within the cell and, thus additional influx during the measurement does not influence the fluorescence. As can be seen in Fig. 4, the fluorescence intensity of the dye drops with increasing laser power supporting the hypothesis that the above described drop in intensity during high power application results from an increase in temperature and not from changes in  $\text{Ca}^{2+}$  concentration.

After the initial drop described above, for the RuR free experiments a significant increase of the fluorescence intensity becomes visible which is significantly steeper for the chelator-

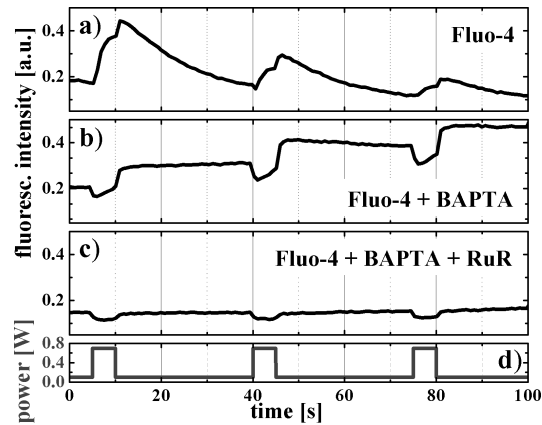


Fig. 3. Fluorescence intensities of single TRPV1 transfected HEK293 cells. The averaged fluorescent signal was recorded (see Fig. 2 for details). Cells were loaded with a) 1 mM Fluo-4,AM, b) 20  $\mu$ M BAPTA,AM and 1  $\mu$ M Fluo-4,AM. c) fluorescence intensity of a cell loaded with 20  $\mu$ M BAPTA,AM and 1  $\mu$ M Fluo-4,AM measured in a solution containing 10  $\mu$ M Ruthenium Red (RuR), a specific blocker of the TRPV1 channel. d) shows the power per fiber of the 1064 nm laser, cells were trapped at 100 mW. Exposure to 700 mW per fiber results in visible deformations and significant heating.

free case. This indicates a drastic rise in the intracellular calcium level in the BAPTA-free experiment and a moderate rise for the chelator containing case. When the laser is switched down to trapping power, another steep increase can be observed as expected due to reduction of the temperature.

In the chelator-free experiment the signal starts decaying after the end of the stretch (Fig. 3a). Since the ion flux due to pumping is proportional to the amount of  $\text{Ca}^{2+}$  ions present in the soma this decay is expected to be exponential in first order for an active pumping process. It is, however, slowed down by the chelating capacity of the dye, as the  $\text{Ca}^{2+}$  ions transiently bound to the relatively large Fluo-4 molecules diffuse much slower through the cell than free  $\text{Ca}^{2+}$  would [44]. The second and third laser pulses in the BAPTA-free experiment show functionally the same characteristics, however, with decreasing amplitudes.

To exclude the involvement of stretch-activated  $\text{Ca}^{2+}$  channels, the experiments were repeated with 10  $\mu$ M  $\text{Gd}^{3+}$ , a potent SAC blocker, in the cell suspension. No significant difference to the fluorescence of untreated cells was observed (data not shown).

In the next step we performed measurements of the relative deformation upon stretching of HEK293 cells to show that with our method the  $\text{Ca}^{2+}$  signaling can be correlated with changes in the mechanical properties of the cell. As can be seen in Fig. 5 the deformation curves change if the  $\text{Ca}^{2+}$  signal is blocked by 20  $\mu$ M BAPTA and 10  $\mu$ M RuR.

### 3.2. Heating in the MOS and TRPV1 activation

During the stretch the liquid in the trap region is heating up as can be seen from Fig. 6. The steep increase of the fluorescence level inside the cells during the stretch phase indicates that this rise in temperature activates the TRPV1 channels, and a pronounced calcium influx is produced (Fig. 3). The smaller amplitudes during the second and third laser pulse in Fig. 3a can be explained by desensitization of the channel [35].

To ensure that heat activates the TRPV1 channel in the MOS, control experiments were performed placing a cell approximately 20  $\mu$ m under the trap region. While increasing the

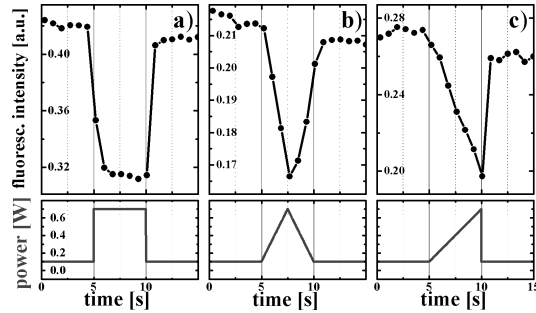


Fig. 4. Cells were loaded with 1  $\mu\text{M}$  Fluo-4 and 20  $\mu\text{M}$  BAPTA,AM. 1  $\mu\text{M}$  Ionomycin, a calcium ionophore, was used to let  $\text{Ca}^{2+}$  enter the cell and saturate the dye as well as the chelator. The application of different laser profiles, a) a rectangular, b) a triangular and c) a saw-tooth shaped pulse, resulted in changes in the fluorescence intensity following the laser power. This is a strong indication that the intensity drop during high laser power application is caused by the temperature increase.

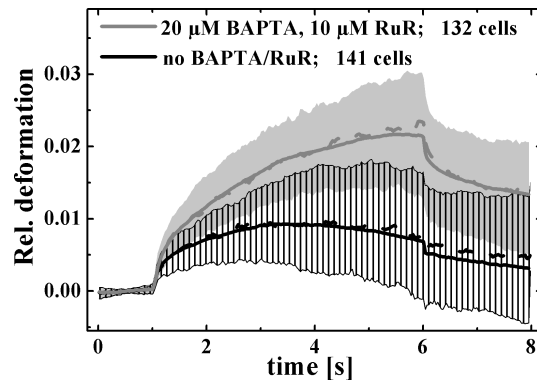


Fig. 5. Relative deformation curves of HEK293 transfected with TRPV1. Mean (solid line) and median (dashed line) of untreated cells (black) and cells treated with 20  $\mu\text{M}$  BAPTA,AM and 10  $\mu\text{M}$  Ruthenium Red (gray). The area around the median marks the quartiles, (black striped for untreated and light gray for BAPTA/RuR treated cells). The graph shows that blocking the  $\text{Ca}^{2+}$  signal correlates with a change in the mechanical properties.

power to 700 mW per fiber did not result in a  $\text{Ca}^{2+}$  influx, 1000 mW produced a strong  $\text{Ca}^{2+}$  wave. As shown in [40] the equilibrium temperature in the vicinity of the trap is lower than in its center. As the activation in this experiment was reached without direct radiation, it proves that the temperature increase due to the laser radiation is enough to activate the temperature sensitive ion channels in the plasma membrane.

Further controls using a solution containing the TRPV1 channel blocker RuR as well as a  $\text{Ca}^{2+}$  free buffer were performed. In both cases approximately 2/3 of the cells still showed an increase in the  $\text{Ca}^{2+}$  level while 1/3 did not, suggesting that release from internal stores plays a role in the experiments (data not shown). A closer investigation of these findings and its impact on cellular mechanics is an interesting application of the presented method.

In Fig. 6 the dynamics of heating and cooling of the trap during a 5 s laser pulse of 700 mW

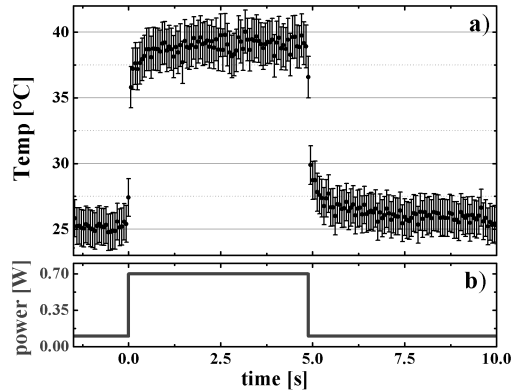


Fig. 6. The temperature during optical trapping and stretching was recorded using the ratio of the intensities of the temperature dependent dye Rhodamine-B and the temperature independent Rhodamine-110 following the method described in [40]. Heating and cooling occurred rapidly within tens of milliseconds.

is shown. During the trapping phases the temperature rises by roughly  $2^{\circ}\text{C}$ , and during the stretch by  $(14 \pm 2)^{\circ}\text{C}$ , reaching a final temperature of  $(39 \pm 2)^{\circ}\text{C}$ . This turned out to be enough to trigger a pronounced  $\text{Ca}^{2+}$  influx. TRPV1 channels are known to have the largest open probability at temperatures above  $\sim 42^{\circ}\text{C}$  [34, 42]. The measured  $(39 \pm 2)^{\circ}\text{C}$  shown in Fig. 6 is the average temperature at the center of the trap without cells or particles. Ebert *et al.* showed that the increase in temperature in the MOS scales with  $(13 \pm 2)^{\circ}\text{C}$  per Watt per fiber [40]. This would give a total temperature increase of  $(18 \pm 3)^{\circ}\text{C}$  for the used 700 mW per fiber, slightly more but within the errors of our measured  $(16 \pm 2)^{\circ}\text{C}$ .

In a control experiment the temperature of the setup was reduced. Below  $(20 \pm 1)^{\circ}\text{C}$  most of the cells did not show an increase in fluorescence intensity during optical stretching. Together with the known temperature threshold of  $\sim 42^{\circ}\text{C}$  this indicates that the trap region heats up slightly more with a trapped cell in it than without. The most probable reason for this effect is a slightly higher absorbance of the laser light by the cell than by the surrounding medium.

It has been shown recently that under normal experimental conditions heating in the MOS does not influence cell viability [45]. In our context it provides a unique tool to activate the heat sensitive TRPV1 channels as soon as the stretch starts.

### 3.3. Chelating $\text{Ca}^{2+}$ signals with BAPTA

In a second experiment the  $\text{Ca}^{2+}$  signal cascade was manipulated by loading the cells with  $20\ \mu\text{M}$  BAPTA,AM. Additionally  $1\ \mu\text{M}$  Fluo-4,AM was added to visualize the  $\text{Ca}^{2+}$  influx during the measurements. The intensity in the cells co-loaded with BAPTA and Fluo-4 drops after the beginning of the laser pulse due to the increase in temperature and rises during the stretch. After the reduction of the laser power a decay of the signal is visible, however, much slower than in the cells not treated with BAPTA. A typical curve is shown in Fig. 3b. In some BAPTA treated cells the  $\text{Ca}^{2+}$  level stayed almost constant or even continued to increase after the laser was switched down to trapping power.

The chelator BAPTA and Fluo-4, which acts as a chelator as well, bind the entering  $\text{Ca}^{2+}$  ions, not permitting them to reach internal  $\text{Ca}^{2+}$  sensors or the pumps reducing the calcium level. Hence, desensitization, depletion of internal stores and pumping of  $\text{Ca}^{2+}$  out of the cell are hindered, explaining the slower decay of the signal and the constant amplitude for subse-

quent stretches. These observations confirm that the co-loading with BAPTA and Fluo-4 hindered  $\text{Ca}^{2+}$  to reach its destination inside the cell.

If additionally the TRPV1 channel is blocked by  $10\ \mu\text{M}$  RuR only a background noise of the fluorescence signal remains, indicating that no measurable amount of  $\text{Ca}^{2+}$  enters the cell (Fig. 3c). This proves that the TRPV1 channel activation is the main pathway by which a calcium influx is produced in the HEK293-TRPV1 model system.

### 3.4. Conclusions

We present a microfluidic system for measuring triggered fluorescent signals in single suspended cells. Cells are held in place and manipulated by optically induced surface forces in the Microfluidic Optical Stretcher (MOS) while the  $\text{Ca}^{2+}$  signal is recorded with confocal laser scanning microscopy (CLSM). The use of the CLSM allows for simultaneous observation of the trapped cells in bright-field images and recording of their fluorescence signals. We show the applicability of our setup using a cell line that was transfected with a heat sensitive ion channel. The heat developed during optical stretching was used to induce a massive  $\text{Ca}^{2+}$  influx. This combination of optical trapping and CLSM opens a wide variety of functional tests using either the deformation or the heat developed in optical traps to induce a change in a fluorescent dye.

An interesting application of the presented setup might be measuring of the restructuring of fluorescently labeled actin or microtubuli upon cellular deformations involving  $\text{Ca}^{2+}$  or other signaling messengers. This could help understand the changes in the cytoskeleton during cancer development contributing to tumor formation and metastasis [12, 46].

In conclusion active cellular responses to heating or deformation mediated by  $\text{Ca}^{2+}$  signaling can strongly influence the mechanical properties of cells. Linear or passive biomechanical models [47–49] will thus not be able to explain the obtained data (see [50] for a recent review on active and passive cell rheology). Observation of signaling cascades might provide a key to understand these active responses of biological cells to external stimuli.

### Acknowledgments

We thank D. Julius (UCSF) for providing the TRPV1 transfected HEK293 cells and A. Fritsch (Univ. Leipzig, Germany) for technical support. The project was funded by the SAB-project 13403 (EFRE) and Agescreeen - Biophotonics 5 Program (funded by the German Federal Ministry of Education and Research (BMBF)) and the graduate school Leipzig School of Natural Sciences – Building with Molecules and Nano-objects "BuildMoNa" of the Universität Leipzig.